

Differences in Morphometric Measures of the Uninjured Porcine Spinal Cord and Dural Sac Predict Histological and Behavioral Outcomes after Traumatic SCI.

KYOUNG-TAE KIM^{†1,2}, FEMKE STREIJGER^{†1}, KITTY SO¹, NEDA MANOUCHEHRI¹, KATELYN SHORTT¹, ELENA BORISOVNA OKON¹, SETH TIGCHELAAR¹, ALLAN FONG¹, CHARLOTTE MORRISON¹, MARTIN KEUNG¹, JENNY SUN¹, ELLA LIU¹,

PETER ALEXANDER CRIPTON^{1,3}, BRIAN KYUNGJIN KWON^{1,4}

1. International Collaboration on Repair Discoveries (ICORD), University of British Columbia (UBC), Vancouver, BC, Canada;
2. Department of Neurosurgery, School of Medicine, Kyungpook National University, Kyungpook National University Hospital, Daegu, South Korea,
3. Orthopaedic and Injury Biomechanics Group, Departments of Mechanical Engineering and Orthopaedics and School of Biomedical Engineering, UBC, Vancouver, BC, Canada,
4. Vancouver Spine Surgery Institute, Department of Orthopaedics, UBC, Vancouver, BC, Canada.

[†] these authors contributed equally to the work.

Kyoung-Tae Kim, M.D., Ph.D.	nskimkt7@gmail.com	Ph: 604-675-8837, Fax: 604-675-8849
Femke Streijger, Ph.D.	streijger@icord.org	Ph: 604-675-8837, Fax: 604-675-8849
Kitty So, B.Sc.	kitty@icord.org	Ph: 604-675-8837, Fax: 604-675-8849
Neda Manouchehri, B.Sc.	nedamanouchehri@gmail.com	Ph: 604-675-8837, Fax: 604-675-8849

Katelyn Shortt	katelyn.shortt@gmail.com	Ph: 604-675-8837, Fax: 604-675-8849
Elena B. Okon, Ph.D.	okon@icord.org	Ph: 604-675-8837, Fax: 604-675-8849
Seth Tigchelaar	sethtigchelaar@gmail.com	Ph: 604-675-8837, Fax: 604-675-8849
Allan Fong	allanfong96@gmail.com	Ph: 604-675-8837, Fax: 604-675-8849
Charlotte Morrison	morrison.charlo@gmail.com	Ph: 604-675-8837, Fax: 604-675-8849
Martin Keung	martinksm@hotmail.com	Ph: 604-675-8837, Fax: 604-675-8849
Jenny Sun	jennysun18@gmail.com	Ph: 604-675-8837, Fax: 604-675-8849
Ella Liu	ella.liu@alumni.ubc.ca	Ph: 604-675-8837, Fax: 604-675-8849
Peter A. Cipton, Ph.D.	Peter.cripton@ubc.ca	Ph: 604-675-8835, Fax: 604-675-8820
Brian K. Kwon, M.D. Ph.D.	brian.kwon@ubc.ca	Ph: 604-875-5857, Fax: 604-875-8223

Corresponding Author (and for Reprints):

Brian K. Kwon, MD, PhD, FRCSC

Canada Research Chair in Spinal Cord Injury

Professor, Department of Orthopaedics, University of British Columbia

6th Floor, Blusson Spinal Cord Centre, Vancouver General Hospital

818 West 10th Avenue, Vancouver, BC, CANADA, V5Z 1M9

PH: 604-875-5857

FX: 604-875-8223

E-mail: brian.kwon@ubc.ca

Key words: Spinal Cord Injury, Porcine model, Ultrasound, Cerebrospinal fluid, spinal cord morphometry

Abstract (max. 250 words)

One of the challenges associated with conducting experiments in animal models of traumatic spinal cord injury (SCI) is inducing a consistent injury with minimal variability in the degree of tissue damage and resultant behavioural and biochemical outcomes. Here, we evaluated how the variability in morphometry of the spinal cord and surrounding cerebrospinal fluid (CSF) contributes to the variability in behavioral and histologic outcomes in our porcine model of SCI.

Using intra-operative ultrasound imaging, spinal cord morphometry was assessed in 7 Yucatan mini-pigs undergoing a weight-drop T10 contusion-compression injury. Bivariate and multivariate *analysis and modeling* were used to identify native morphometric determinants of inter-animal variability in histological and behavioral outcomes.

The measured biomechanical impact parameters did not correlate with the histologic measures or hindlimb locomotor behavior (Porcine Thoracic Injury Behavior Scale). In contrast, clear associations were revealed between CSF layer morphometry and the amount of white matter and tissue sparing. Specifically, the dorso-ventral diameter of the dural sac and ventral CSF space were strong predictors of behavioral and histological outcome and together explained $\geq 95.0\%$ of the variance in these parameters. Additionally, a dorso-ventral diameter of the spinal cord less than 5.331 mm was a strong contributing factor to poor behavioral recovery over 12 weeks.

These results indicate that inter-animal variability in cord morphometry provides a potential biological explanation for the observed heterogeneity in histological and behavioral *outcomes*. Such knowledge is helpful for appropriately balancing experimental groups, and/or varying impact parameters to match cord and CSF layer dimensions, for future studies.

INTRODUCTION

Human spinal cord injuries (SCI) typically occur with the fracturing or dislocation of the spinal column, which then violently imparts a complex set of mechanical forces to the spinal cord. While the biomechanical mechanisms of injury are quite varied,¹ the spinal cord conceptually suffers a blunt “contusive” force followed by some degree of sustained compression. To represent this in the laboratory setting, many contusion-type injury models have been developed.² In such contusion models of SCI, there is inevitably an undesirable degree of variability in histologic and behavioral outcomes, even when utilizing well-established contusion devices and attempting to induce as consistent an injury as possible. This variability can preclude the ability to detect a small beneficial effect of a potential therapeutic intervention, making it difficult to optimize translationally important variables such as dose and therapeutic window. Hence, researchers typically endeavour to understand and minimize variability through the control of experimental variables, and to mitigate bias with randomization of large numbers of animals.

In rodent or other small animal models of SCI, researchers may manage such variability by enrolling large numbers of animals and utilizing tight inclusion/exclusion criteria around the biomechanical parameters of injury such as the contusion displacement or impact force.^{3,4} In such small animal models, variations between animals in the native morphometry of the spinal cord itself are relatively modest. However, in larger animal models such as pigs and primates, there may be considerably greater variability in the morphometric characteristics of the spinal cord and surrounding cerebrospinal fluid (CSF) space to consider.⁵ Because large animal and primate species are so expensive to utilize in SCI modeling (relative to rodents) and because it is always desirable to reduce the number of animals that must be used in each study, understanding how such morphometric characteristics influence outcome after traumatic SCI is important for minimizing variability and conducting experiments in an efficient and cost-effective manner and such that the number of animals used is minimized.

Over the last few years, several groups have utilized pigs to establish SCI models, with injury to the cord induced by contusion,⁶⁻⁸ transection,^{9,10} and static compression.¹¹⁻¹³ Our

Yucatan minipig model of SCI uses a weight-drop device to induce a blunt contusive injury with additional sustained extra-dural compression.⁶ In this early work, we showed how motor recovery and tissue damage were influenced by the height of the weight drop – with higher severity injuries intuitively occurring with the greater heights at which the impactor was dropped. After initially describing this model in 2013,⁶ we have applied it to a number of poorly understood questions of clinical importance that were best investigated with a large animal model; and have characterized the resultant histological damage, inflammatory response, metabolic and hemodynamic impairments, and long-term hindlimb locomotor deficits.¹⁴⁻¹⁹ Furthermore, we have investigated the potential for medical-evacuation-associated vibration (eg ambulance or helicopter vibration) to exacerbate pathologies or outcomes after SCI¹⁶ and evaluated current and novel treatment regimens such as vasopressor therapy¹⁸ and intravenous infusion of magnesium chloride within a polyethylene glycol formulation (AC105).¹⁹

During these studies, we have observed relatively large differences in cord diameter and CSF space around the spinal cord at the T10 region where the injury occurs. The importance of CSF in distributing the direct impact across and along the spinal cord has been recognized by various studies.^{20,21} Intriguingly, recent papers have highlighted that while the spinal cord is indeed protected by fluid, the protection is subject to variations with differences in size of the subarachnoid space.²¹⁻²³ Persson and colleagues²¹ propose that slight variations in the dorso-ventral thickness of the subarachnoid space of only a few millimetres, such as between human vertebral levels, has a substantial effect on the spinal cord deformation during trauma, and thus may give different results in terms of final neurological deficit. It has been reported that individual variation in spinal cord size and CSF layer thickness in humans²⁴ and large animals^{21,25} can be substantial and this is consistent with our own observations in our Yucatan SCI model. For this reason spinal canal diameters are used to estimate SCI risk for contact sports in the so-called Torg Ratio.^{26,27} This indirect evidence from the biomechanics of human SCI also implicates cord and CSF layer morphometry as determinants in the resulting severity of SCI.

These studies suggest that native differences in the morphometry of the spinal cord, CSF layer and spinal canal may contribute to the variability in final histological and

behavioral outcome induced by SCI in our pig model but, as yet, this effect has not been quantitatively established. The purpose of this study was therefore to evaluate the relationship between pre-SCI measurements of the spinal cord morphometry and CSF layer thickness and the resultant severity of injury in this pig model. We aimed to determine whether quantitative differences in spinal cord and CSF layer morphometry would influence the histological and behavioral outcome after a contusive/compressive SCI delivered through weight drop. To our knowledge, no previous *in-vivo* studies have investigated this relationship in a large animal model of SCI.

METHODS

All animal protocols and procedures employed in this study were approved by the Animal Care Committee of the University of British Columbia (UBC) and were compliant with the policies of the Canadian Council on Animal Care and the US Army Medical Research and Materiel Command (USAMRMC) Animal Care and Use Review Office (ACURO).

Animal preparation and spinal cord exposure

Seven female miniature Yucatan pigs (Sinclair Bio-resources, Columbia, MO; weighting: 19.5-34.0 kg) were endotracheally intubated after being anesthetized with intramuscular Telazol (5 milligrams/kg [mg/kg]) and Xylazine (1 mg/kg). Anesthesia was induced using Propofol (2 mg/kg), Fentanyl (10 µg/kg), and Ketamine (11 mg/kg) and maintained using Propofol (8 mg/kg/hr), Fentanyl (12 µg/kg/hr), and Ketamine (11 mg/kg/hr) through a continuous rate infusion (CRI) with a ventilator rate of 10-12 breaths/minute and a tidal volume of 12-15 milliliters/kilogram (ml/kg; Veterinary Anesthesia Ventilator model 2002, Hallowell EMC, Pittsfield, MA). Pigs were given intravenous (IV) cefazolin (15 mg/kg) as a prophylactic antibiotic and an intramuscular (IM) injection of Ketoprofen (3 mg/kg) for analgesia before surgery as well as a maintenance IV solution of 1.25% dextrose during surgery. Standard monitoring was performed during the procedure, including measurement of the animal's heart rate, respiratory rate, blood pressure, end tidal carbon dioxide, inspired and expired isoflurane levels, and oxygen saturation (pulse oximeter 8600V, Nonin Medical Inc., Markham, ON, and Cardell MAX-12HD Veterinary Monitor, Paragon Medical Supply, Inc., Coral Springs, FL). We employed a heating pad to achieve a

target rectal temperature of 37.0–38.0°C (T/Pump, Gaymar Industries, Inc., Orchard Park, NY).

In a prone position, a 13 cm dorsal midline incision was made between the thoracic (T) spine levels T7 and T14. Using monopolar electrocautery (Surgitron, Dual Frequency RF/120 Device; Ellman International, Oceanside, NY), we exposed the spinous processes, laminae, and transverse processes at the T8 through T13 levels. The T9, T10, and T11 pedicles were cannulated and instrumented with 3.5 x 25 mm polyaxial screws (Vertex screws, Medtronic, Memphis, TN). A laminectomy was performed at the T8 through T11 levels, and a circular window was made with a minimum diameter of 1.2 cm to expose the dura and the spinal cord.

Intra-operative ultrasound imaging of the uninjured spinal cord

Ultrasound imaging was utilized to evaluate the pig's uninjured spinal cord and its surrounding structures (**Figure 1A**). The hand-held probe (L14-5/38, 38 mm linear array probe, Ultrasonix RP; BK Ultrasound, Richmond, BC, Canada) was kept about 5 to 10 mm away from the spinal cord. To obtain proper images a layer of saline between the probe head and cord tissue had to be maintained continuously during scanning. One image of the uninjured spinal was captured in both the coronal and mid-sagittal plane at the T10 level (planned level of impact; described in detail below).

SCI and post-operative care

In an attempt to reduce inter-animal *variability* and *standardize* the testing method, the SCI surgical procedure included spinal cord stabilization by using rigid vertebral rods (to mitigate uncontrolled deflection of the vertebral column), usage of breath-hold procedure during impact (to minimize respiratory motion of the spinal cord), and establishment of consistent starting points for the injury and impactor alignment.

A T10 SCI was induced by dropping a 50 g impactor from a height of 20 cm above the dorsal surface of the spinal cord via a fixed guiderail. To simulate “sustained” compression, immediately after the drop, an additional 100 g weight was added onto the impactor (total 150 g) and maintained on the contused spinal cord for 5 minutes. Direct measurements of

impact force and displacement were recorded by a calibrated load cell located within the impactor tip and further analyzed using Labview software (National Instruments Corporation, Austin, TX) (**Table 1**).

After SCI, the incision was closed and the animal was recovered. Fentanyl was administered via continuous rate infusion to control for post-surgical pain. Animals were observed in individual recovery shelters for 7 days post-surgery. Once the animal regained the ability to empty their own bladder, approximately 7-10 days after SCI, the urinary catheter was removed and animals were pair-housed on sawdust bedding.

Behavioral outcome

The Porcine Thoracic Injury Behavior Scale (PTIBS) was used to assess hindlimb recovery.⁶ Briefly, PTIBS classifies hindlimb locomotor function using a score ranging from 1 (absent hindlimb movement) to 10 (normal walking). The PTIBS score categories are as follows: scores of 1–3 define degrees of "hindlimb dragging", scores of 4–6 define degrees of "stepping" or "weight-bearing" ability, and scores of 7–10 define degrees of "walking" ability. To assess the PTIBS score, the animal's walking behavior was recorded with three high-definition camcorders placed behind the animal. Based on the recorded hindlimb and hip movements, a PTIBS score is determined. Baseline behavior was recorded one week before surgery. Weekly behavioral assessments resumed one week after surgery and were recorded for a total 12 weeks. All videos were scored by two independent, blinded observers.

Histological outcome

At 12 weeks after SCI, spinal cords were harvested, fixed in 4% paraformaldehyde, processed for cryoprotection in gradually increasing concentrations of sucrose. The segments of the spinal cord were embedded in optimal cutting temperature (OCT) compound, cut in 20 μ m and mounted on the microscopic slides. For histological evaluation of tissue sparing, spinal cord cross-sections were stained with eriochrome cyanine (EC; Sigma-Aldrich, St. Louis, MO) as described previously.²⁸ A Zeiss Axiolmager M2 microscope (Carl Zeiss Canada Ltd., Toronto, ON, Canada) was used to capture images of

EC-stained sections (5x objective) at 800 μm intervals throughout the lesion site. Images were analyzed using Zen Imaging Software (Carl Zeiss Canada Ltd., Toronto, ON, Canada). Quantification of the lesion area was performed at 800 μm intervals from 13.6 mm caudal to 13.6 mm rostral to the epicenter. Percentage (%) spared tissue was recorded by manual tracing of the spinal cord perimeter and spared tissue for each image captured.⁶ Spared white matter and gray matter percentages were calculated by dividing the area of spared white or gray matter by the total area of the spinal cord in a given section. Total percent spared tissue was calculated by taking the summation of spared white and gray matter and dividing that value by the total area of the spinal cord on its respective cross-section.

Ultrasound measurements of CSF and spinal cord morphometry

Ultrasound images were analyzed using Image J software (Public Domain, <http://rsb.info.nih.gov/ij/>) to determine the following variables: CSF_D : dorsal thickness of the CSF layer; CSF_V : ventral thickness of the CSF layer; SC_{DV} , dorso-ventral thickness of the spinal cord; SC_{TR} , transverse width of the spinal cord; DS_{TR} : transverse width of the dural sac; DS_{DV} : dorso-ventral thickness of the dural sac; SC_{area} : cross-sectional area of the spinal cord; DS_{area} : cross-sectional area of the dural sac; SC_{area}/DS_{area} : cross-sectional area of spinal cord to dural sac ratio (**Figure 1**). All parameters were measured in triplicate by two observers.

Statistical analysis

In the present study, numerical variables were presented as mean \pm standard error of the mean. PTIBS scores were divided into two time epochs after injury, week 2-3 and week 10-12, which represent an early and late measure for behavioral recovery following SCI. Average values and max values for PTIBS score were calculated for each animal within week 2-12 (behavioral indicator of the recovery over time), and week 10-12 (final behavioral outcome). Histological data on the amount of spared white matter, grey matter or total tissue was assessed at 12 week post-SCI and calculated as the area under the curve over the region from 13.6 mm rostral to 13.6 mm caudal to the site of injury.

The data was analyzed in four stages, which include: 1) Principal component analysis (PCA) with varimax rotation, 2) Spearman correlation, 3) Stepwise regression analysis, and 4) Classification and Regression Tree (CART) *analysis*. All tests were two-tailed, with a significance level set at $\alpha=0.05$. All statistical analyses were performed using XLSTAT 16.9 software. Principle components (PCs) were retained using 4 criteria: 1) the Kaiser rule, retaining PCs with eigenvalues >1.0 , 2) Scree plot, and 3) the over-determination of the factors, retaining factors with at least 3 loadings above 0.4. PCs meeting all three criteria were examined. To identify pre-SCI predictors of behavioral and histological outcome, a *stepwise regression analysis was performed* using the probability to enter = 0.05 and probability to remove = 0.05. Spearman correlation coefficients were used to test for associations between the various biomechanical parameters, spared tissue (calculated as the area under the curve), behavioral outcome (PTIBS), and the morphometric measurement of the spinal cord and surrounding.

Two separate multivariable logistic regression models with stepwise selection procedures were performed to identify potential predictor(s) of histologic and behavioral outcome at week 12. Baseline values for cord morphometry, mechanical impact parameters (force, displacement, impulse and velocity), body weight and age at surgery were entered as independent (predictor) variables to predict the dependent (predicted) variable, e.g. histology (total sparing, or TS) and behavioral outcome (PTIBS).

Stepwise selection is considered a variation of forward selection and backward elimination. At each step in the analysis the predictor variable that contributes the most to the prediction equation in terms of increasing the multiple correlation, R, is entered first. After each step in which a variable is added, all candidate predictor variables in the model are checked to see if their significance has been reduced below the specified tolerance level. In this way it is possible to understand the contribution of the previous variables now that another variable has been added. Variables can be retained or deleted based on their statistical contribution. If a non-significant variable is found, it is removed from the model. When no additional predictor variables add anything statistically meaningful to the regression equation, the analysis stops.

In our study, a significance level of 0.05 was defined to allow predictor variables into the regression equation, and a significance level of 0.05 was defined for a predictor variables to stay in the model as other parameters were introduced.

RESULTS

Pre-SCI morphometric measurements

Ultrasound was performed to evaluate the morphometric measures of the uninjured spinal cord and surrounding (**Figure 1**). The parameters analyzed were the dorso-ventral thickness of the spinal cord (SC_{DV}) and dural sac (DS_{DV}), transverse width of the spinal cord (SC_{TR}) and dural sac (DS_{TR}), ventral and dorsal thickness of the CSF layer (respectively, CSF_V and CSF_D), and the cross-sectional area of the spinal cord (SC_{area}), dural sac (DS_{area}) and CSF space (CSF_{area}). All parameters were measured in triplicate by two observers. The three measurements of each parameter were averaged to obtain one value per parameter per observer. The intra- and inter-rater reliability coefficient was between 0.92 and 0.99 for measurements in both transverse and dorso-ventral planes (95% CI; **Supplementary Table 1**).

At the T10 level, SC_{DV} and SC_{TR} were fairly constant between the 7 animals, with an average of 5.34 ± 0.28 mm and 6.70 ± 0.25 mm respectively (**Table 2**). The ratio between the cross-sectional area of the spinal cord to that of the dural sac (SC/DS) ranged from 0.44 to 0.68. In other words, when viewed in cross-section, the spinal cord occupied between 45 and 70% of the intrathecal space. Interestingly, the body weight of the animal (**Table 2**) was not a determinant for the size of the spinal cord or dural sac (Spearman correlation, $p > 0.05$). In the prone position, both CSF_V and CSF_D varied considerably between animals, ranging from 0.50 mm to 1.67 mm for CSF_V and 1.02 mm to 2.47 mm for CSF_D respectively. Dorso-ventral symmetry in the location of the spinal cord within the dural sac was found in approximately 42% of the animals (animal #2-4), with the CSF_D/CSF_V ratio close to 1. Animal #1 and #7 demonstrated a more dorsal position of the spinal cord within the dural sac (CSF_D/CSF_V ratio #1: 4.96, #7: 2.04), while #5 and #6 showing a more ventral position (CSF_D/CSF_V ratio #5: 0.68, #6: 0.76). In the transverse direction, CSF space was always symmetrical.

Mechanical injury parameters

Subsequently, all animals received a contusion injury with the 50 g impactor dropped from a height of 20 cm, followed by 5 minutes of sustained compression. *Despite* our attempts to standardize all aspects of the experimental SCI, we still observed variability of approximately 24% in the peak force between animals (**Table 1**). On average, the peak force applied to the exposed spinal cord was 3135 ± 282 kdynes with an impulse of 10.94 ± 0.43 kdyne*sec. The impactor tip traveled 4.89 ± 0.16 mm from initial contact with the exposed dura with a velocity of 1782 ± 44 mm/sec at impact. The individual biomechanical impact parameters of the animals are presented in **Table 1**.

Behavioral and histological outcomes following SCI

PTIBS scoring was performed to assess changes in gross locomotor performance following contusion injury (**Figure 2**). Prior to contusion surgery, all animals achieved a baseline score of 10, indicating normal locomotion and hindlimb function. When first tested after SCI, the overall pattern of behavioral outcome revealed a clear initial deficit with a PTIBS score of ≤ 3 , indicating varying degrees of hindlimb movements with or without weight bearing extension, which lifts the *rump* and *knees* transiently *off the floor* (**Figure 2**). Over the long-term course of recovery (12 weeks), two recovery patterns could be distinguished within the injury group: those in which the initial deficit persisted over time, e.g. PTIBS scores remained ≤ 3 by the final week of the study (animal #1, #3, #4, #7); and those which recovered from the initial deficit fairly well to a PTIBS of 4-5 (animal #2, #5, #6), indicating that the animals are moving from “dragging” to the earliest stages of “stepping”.

In order to quantify the extent of tissue sparing at the lesion epicenter as well as the rostro-caudal spread of the injury, quantitative image analysis was carried out on serial sections stained with eriochrome cyanine R. Tissue-sparing data is presented in **Figure 3**. By 12 weeks after injury, substantial spinal cord damage is present at the lesion *epicenter*, affecting both white (WMS: 0 to 12.0%) and gray matter (GMS: 0%). With increased distances from the epicenter, the amount of total preserved *tissue significantly increased*. Rostrally, the extent of visible total tissue damage tapered off rapidly and on average at -

9.5 ± 0.88 mm (range: -7.2 to -13.6) from the epicenter centre the spinal cords appeared visibly undamaged (TS: >97%) for all animals. While for the majority of the animals a similar pattern was evident caudally to the epicenter, in 43% of the animals (3 out of the 7) tissue damage extended to the very last section analyzed (13.6 mm).

Morphometric factors affecting variability in impact parameters, histology and function after SCI

PCA analysis was conducted to determine which variables clustered together (known as principal components, PC) as well as their contributions to overall outcome variance. PCA analysis revealed a three-dimensional PC outcome space, accounting for 92.08% of the variance in the data set. The three PCs that explained the vast majority of the variance within the data are presented in **Table 3**. To understand how individual variables related to the PCA patterns, the correlation (i.e. factor loading) of each variable is reported. Loading magnitude is illustrated by the intensity of the color (Blue reflects negative and red reflects positive loadings).

The first dimension (D1), accounting for 43.40 % of the variance in the dataset and an eigenvalue of 10.608, represented a positive association between histological sparing variables (WMS, GMS, TS), baseline dural sac morphometry (DS_{TR} , DS_{DV} , DS_{area} , CSF_D , CSF_{DV} , CSF_{area}) and displacement. It is noteworthy that $PTIBS_{10-12}$ did not strongly load on D1, although this dimension was heavily loaded with histological variables.

The second dimension (D2) explaining 25.25% of the variance, with an eigenvalue of 5.877, largely represented a negative association between biomechanical factors (impact force, impulse, velocity) and the animal's physical status at the time of surgery (age and bodyweight). Finally, the third component was predominated by a positive association between behavioral recovery variables ($PTIBS_{2-12}$, $PTIBS_{10-12}$), and spinal cord morphometry (SC_{DV} and SC_{area}). This component accounted for 23.79% of the data variance with an eigenvalue of 1.930.

Based on these PCA results, the association between the variables in D1, D2 and D3 were examined more closely by running a univariate Spearman correlation coefficient

analysis (Table 4). DS_{DV} , DS_{area} , CSF_{area} strongly correlated with measures of tissue sparing (WMS, GMS, and TS), with *r-values* ranging between 0.786-0.964. The variables displacement ($r:0.929$, $p=0.007$) and CSF_{DV} ($r:0.857$, $p=0.0$) strongly correlated with GMS, however the correlation with WMS or TS was not significant ($p>0.066$). Moreover, there was a strong correlation between SC_{area}/DS_{area} and GMS ($r=-0.786$, $p=0.048$). The correlation between CSF_D and the other tissue sparing parameters was not statistically significant ($p>0.236$). Peak force and velocity strongly correlated with age (Force; $r=-0.857$, $p=0.024$; Velocity; $r=-0.786$, $p=0.048$) and body weight of the animal (Force; $r=-0.855$, $p=0.024$; Velocity; $r=-0.873$, $p=0.012$), i.e. younger animals or lower bodyweights resulted in higher impact forces and velocities. Both behavioral outcome parameters (PTIBS₂₋₁₂ and PTIBS₁₀₋₁₂) strongly correlated with SC_{DV} , with *r-values* of 0.793 ($p=0.048$) and 0.852 ($p=0.034$), respectively. The correlation between SC_{area} and the behavioral outcome measures (PTIBS₂₋₁₂, PTIBS₁₀₋₁₂) was not statistically significant ($p>0.200$).

Thus, with either bivariate or multivariate analysis, there appeared to be a clear relationship between post-SCI outcome measures (PTIBS and tissue sparing) and the morphometry of the spinal cord and surrounding intrathecal space, which could be measured intra-operatively with ultrasound. Next, we sought to determine whether any single variable or combination could provide reliable behavioral or histological outcome determination. A *stepwise multiple regression* model containing all the biomechanical and morphometric measures revealed that changes in DS_{DV} , CSF_V and impactor displacement were the three most influential predictors for white matter sparing ($R^2: 0.992$; Adjusted $R^2: 0.985$; $Pr(>F): 0.001$). DS_{DV} alone explained 77.3% of the variance in white matter sparing (standardized $\beta= 0.951$; 95% CI: 0.625-1.276; $p=0.003$), while the remaining CSF_V and displacement parameter explained an additional 17.7% (standardized $\beta= 0.561$; 95% CI: 0.366-0.756; $p=0.003$) and 4.2% respectively (standardized $\beta= -0.430$; 95% CI: -0.763—0.097; $p=0.026$). The two variables, DS_{DV} (standardized $\beta= 0.689$; 95% CI: 0.411-0.968; $p=0.002$) and CSF_V (standardized $\beta= 0.425$; 95% CI: 0.146-0.703; $p=0.013$), were also found to be significant predictors of accumulative spared tissue and together explained 97.1% of the variance ($Pr(>F): 0.001$). With each 1-mm increase in DS_{DV} , the amount of white matter or accumulative tissue sparing increased respectively 8.5% and 6.5%.

The stepwise method regression analysis additionally revealed that the change in impact force and displacement was a poor predictor of behavioral recovery over 12 weeks, while the change in SC_{DV} showed a moderate, but significant prediction (PTIBS₁₀₋₁₂ R^2 : 0.682; Adjusted R^2 : 0.619; $Pr(>F)$: 0.022; PTIBS₂₋₁₂ R^2 : 0.777; Adjusted R^2 : 0.732; $Pr(>F)$: 0.009). As mentioned earlier, within the injury group two distinct PTIBS recovery patterns could be distinguished: (1) those in which the initial deficit persisted over time, and (2) those which recovered from the initial deficit fairly well. Hence, we determined whether pre-SCI morphometric measures were different between those animals which experienced PTIBS improvement over time versus those animals who did not. Classification and regression tree (CART) analysis identified a decision tree defined by three nodal points that stratified the cohort into two groups (**Figure 4**). The tree showed that the first split was based on SC_{DV} , and the CART analysis generated the cut-off to be 5.331 mm for 100% correct *classification into* target groups of poor recovery (n=4) and significant recovery (n=3). Thus, besides anatomical outcomes, these analyses suggest that pre-SCI morphometric measures of the spinal cord can additionally predict the likelihood of regaining stepping ability.

Discussion

The development of standardized *in-vivo* mouse and rat models of traumatic SCI has been invaluable to the SCI field for the testing of novel therapeutic strategies. Researchers typically strive to minimize variability within the experimental design of such pre-clinical studies through the tight control of animal features (e.g. strain, gender, weight), experimental setup (e.g. anaesthesia, temperature, pre- and post-injury housing and care, surgical techniques) and biomechanics of injury (e.g. utilization of standardized, calibrated contusion or compression devices). Through the minimization of variability, it is expected that consistent and comparable injury severities can be induced amongst the animals and the detection of small, yet statistically significant, therapeutic effects may be possible.

By employing measures to minimize experimental variability, several rat and mouse models of contusion injury have demonstrated a positive *correlation between behavioral recovery and* the extent of *spared* tissue following contusion injury.²⁹⁻³⁶ However, it is

recognized that even with these tightly controlled experimental conditions, variability often necessitates the exclusion of up to 10% (or even more) of the animals in order to isolate distinct biomechanical groups.^{3,4} Due to the tremendous financial cost associated with SCI experimentation in large animal species such as the pig, it is critically important to recognize the sources of experimental variability and minimize them to be able to conduct studies with a financially-realistic number of animals and to minimize the number of animals used. Given the cost of each animal, the animal care required and the desire to minimize the use of animals, it is extremely inefficient to have to exclude an animal if the biomechanical parameters fall outside a given range, or even add additional animals to the cohort to make up for it.

In our initial characterization of the model,⁶ we felt that while we might have impact variability related to the actual contusive injury and arising from morphometric differences, from dropping a 50 g weight from a specific height, that this would be ultimately “blunted” by subsequently adding 100 g for 5 minutes to induce sustained compression that simulates pressure from bone fragments or vertebrae in clinical SCI. Based on the consistent PTIBS scores that we observed within each injury severity group, this appeared to be true. However, in our subsequent experience with this model, we have continued to observe variability in the initial contusion impact, and we also noted even on visual inspection during surgery that there were quite noticeable differences in the size of the spinal cord and the extent of CSF around it at the T10 level. This study was therefore undertaken to try to understand the relationship between these native anatomical variations and the variability in the various measures of the impact and subsequent outcome.

While a correlation was found between the amount of tissue sparing (white matter and total sparing) and the PTIBS₂₋₁₂ outcome, the non-significant correlation between histology and the final PTIBS outcome (PTIBS₁₀₋₁₂) was somewhat unexpected. In agreement with this, behavioral function and histology did not co-load on the same dimension in PCA. When considering each time point separately, the correlation between spared tissue and PTIBS was statistically significant at week 3, 4 and 6 (unpublished data). This observation suggests that the behavioral changes over time may mirror distinct

biological mechanisms. For example, behavioural recovery acutely after SCI may be directly related to changes associated with tissue sparing and sparing of associated spinal tracts, whereas recovery in the subsequent weeks may be the results of endogenous plasticity associated with axonal sprouting in and around the spared area, for example. We acknowledge that the EC staining provides only a general perspective of tissue sparing and does not yield information about axonal sparing or sprouting/plasticity. Resolving the drivers of complex behavioral outcomes in SCI would require *more extensive histological* evaluation, such as axon tracing, and/or immunohistochemistry for 5HT or SERT.

As observed in our cohort of animals, contusion impact with a pre-defined drop height of 20 cm to the spinal cord does not necessarily cause identical histological damage or behavioral deficits in all animals. *Our PCA results partly confirmed* previous research,³⁷ as we showed that of the various mechanical parameters, tissue displacement dictated the observed differences in the histopathological outcome of SCI. While Kearny and colleagues reported in their study that the product of velocity x displacement was the best predictor of SCI outcome severity as measured by function, it is noteworthy that velocity and displacement were independently controlled in the Kearney study.³⁷ The weight drop model as used in our study delivered a “standardized” velocity (dictated by gravity and the constant height above the cord from which we dropped the weight); while force and tissue displacement response during the impact were prescribed by the geometric, material property and other characteristics of the cord being impacted during the impact. Therefore it is expected, since we were not varying velocity, that the severity would be dictated by cord displacement and this is what we observed.

While DS_{DV} , displacement, and tissue sparing loaded highly on a single dimension in PCA with all variables loading positively, a seemingly contradictory result was found with the multiple regression method, which showed a small negative contribution of displacement to the regression equation to predict total spared tissue. It should be noted however, that there are fundamental differences between the multiple regression and PCA method and that they examine slightly different questions. The aim of the PCA is to search for global patterns in the independent variables that explains most of the variation in the data and does not require a dependent variable. In the interpretation of PCA, factor

loadings are equivalent to bivariate correlations between the observed variables and the components.

Multiple regression on the other hand is used to determine whether one variable can be predicted from a combination of other variables. When predictor variables are correlated, beta coefficients may mislead the interpretation of how different predictors influence the dependent variable, because, they are based on a predictor's relation with the dependent variable, as well as with all other predictors in the model.³⁸ Thus, a predictor's contribution to the regression equation may be negative even when its relationship to the dependent variable is positive, which may be inappropriately interpreted as a negative relationship with the dependent variable.³⁹ Thus, comparing the results of PCA and multiple regression analysis must be interpreted cautiously as the computations made rely on different methodologies.

The smaller but still significant variation in force, and impulse appeared to be highly sensitive to the non-SCI variables of body weight and age at the time of the injury. The fact that age and weight clustered together with the various impact variables suggest that they have a special significance in the SCI biomechanical signature, beyond the other variables measured. Reasons underlying this correlation are difficult to ascertain. However, one explanation may be age related changes in spinal cord tissue stiffness. Arani and colleagues found a moderate inverse linear correlation between age and stiffness in the cerebrum of healthy adults, although such correlation was not found in the cerebellum.⁴⁰ Likewise, previous research indicated that CNS stiffness was likely to increase during adolescence in rats.⁴¹ Furthermore, Clarke and colleagues reported that stress-relaxation behavior in spinal cord tissue between adult and neonate rats differed significantly.⁴² Besides CNS tissue stiffness, age and bodyweight also likely contributed to changes in tissues such as articular cartilage, bone, ligaments, adipose tissue and musculature. While all these factors could in theory influence the impact, in our study a cohort with a relatively narrow age and body weight range was used and further exploration is needed to fully understand the causal mechanisms.

PCA also indicated a robust clustering of variance of spinal cord size and behavioral recovery. In line with this, spinal cord size was also the most influential variable predicting behavioural outcome with the multiple regression analysis. Such relation was also demonstrated using a classification tree approach with behavioral recovery converted into a two category scale (poor recovery vs significant recovery). This connection is likely due to intrinsic differences in the composition of cord tissue itself. Since spinal cord size did not cluster on D2, its variation is likely related to changes in anatomical features contributing to the intrinsic mechanical properties of the spinal cord while under compression. Intriguingly, previous research has indicated a notable dependence of the magnitude of spinal cord compression under a given load with variances in the cross-sectional surface ratio of gray matter (GM) over white matter (WM).²⁰ While in the current study we did not measure axial dimensions of GM and WM, our previous research using sham control pigs¹⁹ revealed that the inter-individual variability at the T10 level was relatively low (4%; unpublished data). It is interesting to note that, despite the low variance between these animals, spinal cord dimensions at the T10 and GM to WM ratio were highly correlated ($r=0.90$), i.e. a larger spinal cord related to lower GM to WM ratios. Thus, the observation linking variances in spinal cord dimension and structure (and the mechanical behavior of the tissue), might explain the observed association between a larger spinal cord size and better functional outcome with PCA in our study.

While outcome severity has been characterized by measuring peak force, displacement, velocity, energy, or impulse-momentum, the variability observed in histological and behavioral outcome between animals in our study could not be explained exclusively on the basis of mechanical impact parameters. In contrast, there appeared to be a clear relationship between outcome measures and dural sac morphometry. The amount of CSF within the dural sac appeared to be the most influential predictor of tissue sparing; with only submillimeter increases resulting in increases in tissue sparing. In particular, the amount of CSF ventral to the spinal cord accounted for much of the residual variability in tissue damage. The observed relationship dural sac/CSF measures and outcome of SCI was an expected result when considering the mechanics of the contusion model used here. The weight drop results in the tip of the impactor interacting with the

dura. The dura, at this time point, is separated from the cord by the dorsal CSF layer and the spinal cord is likewise separated from the posterior surface of the vertebral body at the injury level by the ventral CSF layer. Then, the impactor must squeeze the dura towards the spinal cord and simultaneously accelerate the spinal cord and displace the ventral CSF. This likely resulted in complex CSF flow patterns ventral, dorsal as well as lateral to the spinal cord. It is clear that the mechanics of CSF flow are complex in nature^{22,43,44} but not all aspects of the CSF flow relevant to the present discussion have been reported. Only when the CSF is displaced both ventral and dorsal to the spinal cord (termed “CSF Obliteration” by Khuyagbaatar and colleagues),⁴⁴ could the impactor apply force directly to the spinal cord and compress it against the posterior aspect of the vertebral body.

The mechanics of the cord/CSF/canal interaction also suggest an explanation for the importance of the ventral CSF layer,⁵ specifically in the present study. We hypothesized that the falling impactor always had enough energy to displace the dorsal CSF layer and to accelerate the cord toward the ventral surface of the spinal canal. CSF ventral to the spinal cord would have the ability to absorb the energy associated with the motion of the incoming cord and impactor proportional to its thickness. A thicker ventral CSF layer would absorb more of the energy associated with the moving impactor and cord and thus there would be less energy remaining to compress the cord against the vertebral body.

During impact, various components of the spinal cord parenchyma, such as endothelial cells, myelinated and unmyelinated axons, glial processes, cell somas, and spinal meninges, will experience diverse extents of mechanical distortion above or below their threshold for irreversible physical disruption. It is damage to these components that result in neurological impairment. Previous studies using animals and human cadavers, as well as computational models, have outlined the influence of CSF on SCI severity.^{21,23,44-47} In a bovine and synthetic model of SCI, researchers have found that increased dimensions of the dural sac or CSF layer associated with a substantial reduction in cord deformation.^{22,23,46} Furthermore, it has been speculated that a thicker fluid layer may reduce the stress or stress fields induced in the injured spinal cord.²² Using a finite element model of the spinal cord, Fradet and colleagues²⁰ demonstrated that when increasing the

ratio of the thoracic spinal cord to CSF from 0.42 to 0.78 (to match human and bovine morphology respectively), a marginal increase in spinal cord compression (3%) was observed; however this slight increase resulted in stress increases of up to 28% in white matter.²⁰ In addition, greater tissue damage has been associated with increased mechanical stress,⁴⁸ implying a possible reduction in the degree of neurological deficit with increased CSF thickness in an *in vivo* situation.

Evaluation of the inter-animal variability in morphometric characteristics of the epidural (or extradural) space, formed between the walls of the vertebral canal and the dura matter, should also be considered in future work. This space contains variable amounts of epidural fat, the subdural venous plexus, spinal arteries and lymphatic vessels, as well as the ligamentum flavum and posterior longitudinal ligament. Notably, such elements can provide spinal motion stability and cushion effect in the spinal cord during impact. Unfortunately, the ultrasound technique as used in the current study did not provide adequate resolution to specifically and accurately identify the epidural space. *A more powerful, higher-frequency ultrasound signal would improve the resolution of our probe and aid in depicting the location of the epidural space.*

Interestingly, there was no correlation between body weight and the physical dimensions of the CSF layer, which indicate that it is not possible to stratify animals pre-operatively based on their weight. Likewise, body weight and age of the animals had no significant correlation to spinal cord cross-sectional area, dorso-ventral thickness, or transverse width. This implies that the size of the spinal cord remained relatively constant within the weight range under consideration (23.5-34.0 kg), despite continuous body growth during the first 5-8 months of age. Such lack of correlation is consistent with previous studies, which demonstrated that changes in cross-sectional diameter of the spinal cord of healthy humans were not associated with body weight change.⁴⁹⁻⁵²

This study is a first step in understanding the heterogeneity in outcome severity in large animal models of SCI, such as the pig. Overall, our results highlight the value of introducing pre-impact ultrasound imaging as part of the SCI protocol in large animal models of SCI. We have demonstrated that the size of the spinal cord and dural sac at the

time of impact are strong contributors to the behavioral and histological outcome. To reduce outcome variability and the number of animals needed, as well as to improve sensitivity for detecting treatment effects in large animal models of SCI, it is thus highly desirable to correct or adjust for size differences in the spinal cord and its surrounding. It could be hypothesized that removing CSF or displacing it in a controlled manner may be effective in reducing the variability induced by size differences. Another way to deal with morphological differences is customizing impact protocols to the size of the animal's spinal cord and thecal space. A key challenge in developing this methodology for a weight drop injury such as ours would be to precisely estimate the drop height to cause a specified injury severity with, say, a large CSF layer and the drop height for the same severity with a small CSF layer. Other approaches, such as pre-stratification of treatment groups and post-statistical correction methods should also be considered in future studies.

In conclusion, our ongoing work with the pig model of SCI has provided important insights into the relationship between inherent anatomic variability in spinal cord morphometry and outcomes after traumatic, experimentally induced SCI. These considerations are important to recognize in order to maximize the utility of these expensive animal models and in the development of future SCI risk criteria to better identify people at increased risk of SCI in contact sports.

Acknowledgement

The authors gratefully acknowledge the tremendous expertise and commitment of the entire team of veterinarians and animal care technicians at the UBC Center for Comparative Medicine (CCM). Their dedication and skill make it possible to conduct these experiments with the utmost in care for the animals. Dr. Kim is supported by the Basic Science Research Program through the National Research Foundation of Korea (NRF) funded by the Ministry of Science and ICT (NRF-2012R1A1A1014361, NRF-2015R1C1A1A01056299). Funding for this study was received from the United States Defense Medical Research & Development Program. Dr. Kwon gratefully acknowledges the support of the Canada Research Chairs program and the VGH & UBC Hospital Foundation.

Author Disclosure Statement

No competing financial interests exist.

References

1. Mattucci, S., Speidel, J., Liu, J., Kwon, B. K., Tetzlaff, W., Oxland, T. R. (2018). Basic biomechanics of spinal cord injury — How injuries happen in people and how animal models have informed our understanding. *Clinical Biomechanics*
2. Hodgetts, S.I., Plant, G.W., Harvey, A.R. (2008) Spinal cord injury: experimental animal models and relation to human therapy, in: *The Spinal Cord: A Christopher and Dana Reeve Foundation Text and Atlas*. C. Watson, G. Paxinos and G. Kayalioglu (eds). Academic Press/Elsevier: San Diego, pps. 209-222.
3. Kloos, A. D., Fisher, L. C., Detloff, M. R., Hassenzahl, D. L., Basso, D. M. (2005). Stepwise motor and all-or-none sensory recovery is associated with nonlinear sparing after incremental spinal cord injury in rats. *Exp Neurol* 191, 251-265.
4. Ghasemlou, N., Kerr, B. J., David, S. (2005). Tissue displacement and impact force are important contributors to outcome after spinal cord contusion injury. *Exp Neurol* 196, 9-17.
5. Salegio, E. A., Bresnahan, J. C., Sparrey, C. J., Camisa, W., Fischer, J., Leasure, J., Buckley, J., Nout-Lomas, Y. S., Rosenzweig, E. S., Moseanko, R., Strand, S., Hawbecker, S., Lemoy, M. J., Haefeli, J., Ma, X., Nielson, J. L., Edgerton, V. R., Ferguson, A. R., Tuszynski, M. H., Beattie, M. S. (2016). A Unilateral Cervical Spinal Cord Contusion Injury Model in Non-Human Primates (*Macaca mulatta*). *J Neurotrauma* 33, 439-459.
6. Lee, J. H., Jones, C. F., Okon, E. B., Anderson, L., Tigchelaar, S., Kooner, P., Godbey, T., Chua, B., Gray, G., Hildebrandt, R., Cripton, P., Tetzlaff, W., Kwon, B. K. (2013). A novel porcine model of traumatic thoracic spinal cord injury. *J Neurotrauma* 30, 142-159.
7. Kuluz, J., Samdani, A., Benglis, D., Gonzalez-Brito, M., Solano, J. P., Ramirez, M. A., Luqman, A., De los Santos, R., Hutchinson, D., Nares, M., Padgett, K., He, D., Huang, T., Levi, A., Betz, R., Dietrich, D. (2010). Pediatric spinal cord injury in infant piglets: description of a new large animal model and review of the literature. *J Spinal Cord Med* 33, 43-57.
8. Islamov, R. R., Sokolov, M. E., Bashirov, F. V., Fadeev, F. O., Shmarov, M. M., Naroditskiy, B. S., Povysheva, T. V., Shaymardanova, G. F., Yakupov, R. A., Chelyshev, Y. A., Lavrov, I. A. (2017). A pilot study of cell-mediated gene therapy for spinal cord injury in mini pigs. *Neurosci Lett* 644, 67-75.

9. Hachmann, J. T., Jeong, J. H., Grahn, P. J., Mallory, G. W., Evertz, L. Q., Bieber, A. J., Lobel, D. A., Bennet, K. E., Lee, K. H., Lujan, J. L. (2013). Large animal model for development of functional restoration paradigms using epidural and intraspinal stimulation. *PLoS One* 8, e81443.
10. Lim, J. H., Piedrahita, J. A., Jackson, L., Ghashghaei, T., Olby, N. J. (2010). Development of a model of sacrocaudal spinal cord injury in cloned Yucatan minipigs for cellular transplantation research. *Cell Reprogram* 12, 689-697.
11. Navarro, R., Juhas, S., Keshavarzi, S., Juhasova, J., Motlik, J., Johe, K., Marsala, S., Scadeng, M., Lazar, P., Tomori, Z., Schulteis, G., Beattie, M., Ciacci, J. D., Marsala, M. (2012). Chronic spinal compression model in minipigs: a systematic behavioral, qualitative, and quantitative neuropathological study. *J Neurotrauma* 29, 499-513.
12. Jones, C. F., Lee, J. H., Burstyn, U., Okon, E. B., Kwon, B. K., Crompton, P. A. (2013). Cerebrospinal fluid pressures resulting from experimental traumatic spinal cord injuries in a pig model. *J Biomech Eng* 135, 101005.
13. Šulla, I., Bačiak, L., Juránek, I., Cicholesová, T., Boldižár, M., Balik, V., Lukáčová, N. (2014). Assessment of motor recovery and MRI correlates in a porcine spinal cord injury model. *Acta Veterinaria Brno* 83, 393-397.
14. Okon, E. B., Streijger, F., Lee, J. H., Anderson, L. M., Russell, A. K., Kwon, B. K. (2013). Intraparenchymal microdialysis after acute spinal cord injury reveals differential metabolic responses to contusive versus compressive mechanisms of injury. *J Neurotrauma* 30, 1564-1576.
15. Streijger, F., Lee, J. H., Chak, J., Dressler, D., Manouchehri, N., Okon, E. B., Anderson, L. M., Melnyk, A. D., Crompton, P. A., Kwon, B. K. (2015). The effect of whole-body resonance vibration in a porcine model of spinal cord injury. *J Neurotrauma* 32, 908-921.
16. Streijger, F., Lee, J. H., Manouchehri, N., Melnyk, A. D., Chak, J., Tigchelaar, S., So, K., Okon, E. B., Jiang, S., Kinsler, R., Barazanji, K., Crompton, P. A., Kwon, B. K. (2016). Responses of the Acutely Injured Spinal Cord to Vibration that Simulates Transport in Helicopters or Mine-Resistant Ambush-Protected Vehicles. *J Neurotrauma* 33, 2217-2226.

17. Streijger, F., So, K., Manouchehri, N., Tigchelaar, S., Lee, J. H. T., Okon, E. B., Shortt, K., Kim, S. E., McInnes, K., Cripton, P., Kwon, B. K. (2017). Changes in Pressure, Hemodynamics, and Metabolism within the Spinal Cord during the First 7 Days after Injury Using a Porcine Model. *J Neurotrauma* 34, 3336-3350.
18. Streijger, F., So, K., Manouchehri, N., Gheorghe, A., Okon, E. B., Chan, R. M., Ng, B., Shortt, K., Sekhon, M. S., Griesdale, D. E., Kwon, B. K. (2018). A Direct Comparison between Norepinephrine and Phenylephrine for Augmenting Spinal Cord Perfusion in a Porcine Model of Spinal Cord Injury. *J Neurotrauma*
19. Streijger, F., Lee, J. H., Manouchehri, N., Okon, E. B., Tigchelaar, S., Anderson, L. M., Dekaban, G. A., Rudko, D. A., Menon, R. S., Iaci, J. F., Button, D. C., Vecchione, A. M., Konovalov, A., Sarmiere, P. D., Ung, C., Caggiano, A. O., Kwon, B. K. (2016). The Evaluation of Magnesium Chloride within a Polyethylene Glycol Formulation in a Porcine Model of Acute Spinal Cord Injury. *J Neurotrauma* 33, 2202-2216.
20. Fradet, L., Arnoux, P.-J., Callot, V., Petit, Y. (2016). Geometrical variations in white and gray matter affect the biomechanics of spinal cord injuries more than the arachnoid space. *Advances in Mechanical Engineering* 8, 168781401666470.
21. Persson, C., Summers, J., Hall, R. M. (2011). The effect of cerebrospinal fluid thickness on traumatic spinal cord deformation. *J Appl Biomech* 27, 330-335.
22. Jones, C. F., Kwon, B. K., Cripton, P. A. (2012). Mechanical indicators of injury severity are decreased with increased thecal sac dimension in a bench-top model of contusion type spinal cord injury. *J Biomech* 45, 1003-1010.
23. Jones, C. F., Kroeker, S. G., Cripton, P. A., Hall, R. M. (2008). The effect of cerebrospinal fluid on the biomechanics of spinal cord: an ex vivo bovine model using bovine and physical surrogate spinal cord. *Spine (Phila Pa 1976)* 33, E580-8.
24. Kameyama, T., Hashizume, Y., Ando, T., Takahashi, A. (1994). Morphometry of the Normal Cadaveric Cervical Spinal Cord. *Spine* 19, 2077-2081.
25. Blight, A. R., Decrescito, V. (1986). Morphometric analysis of experimental spinal cord injury in the cat: the relation of injury intensity to survival of myelinated axons. *Neuroscience* 19, 321-341.
26. Pavlov, H., Torg, J.S., Robie, B., Jahre, C. (1987). Cervical spinal stenosis: determination with vertebral body ratio method. *Radiology* 164, 771-775.

27. Torg, J.S. (2002) Cervical spinal stenosis with cord neurapraxia: evaluation and decisions regarding participation in athletics. *Curr Sports Med Rep*, 1, 43-36.
28. Rabchevsky, A. G., Fugaccia, I., Sullivan, P. G., Scheff, S. W. (2001). Cyclosporin A treatment following spinal cord injury to the rat: behavioral effects and stereological assessment of tissue sparing. *J Neurotrauma* 18, 513-522.
29. Streijger, F., Beernink, T. M., Lee, J. H., Bhatnagar, T., Park, S., Kwon, B. K., Tetzlaff, W. (2013). Characterization of a cervical spinal cord hemicontusion injury in mice using the infinite horizon impactor. *J Neurotrauma* 30, 869-883.
30. Basso, D. M. (2000). Neuroanatomical substrates of functional recovery after experimental spinal cord injury: implications of basic science research for human spinal cord injury. *Phys Ther* 80, 808-817.
31. Behrmann, D. L., Bresnahan, J. C., Beattie, M. S., Shah, B. R. (1992). Spinal cord injury produced by consistent mechanical displacement of the cord in rats: behavioral and histologic analysis. *J Neurotrauma* 9, 197-217.
32. Bresnahan, J. C., Beattie, M. S., Todd, F. D., Noyes, D. H. (1987). A behavioral and anatomical analysis of spinal cord injury produced by a feedback-controlled impaction device. *Exp Neurol* 95, 548-570.
33. Dunham, K. A., Siriphorn, A., Chompoonpong, S., Floyd, C. L. (2010). Characterization of a graded cervical hemicontusion spinal cord injury model in adult male rats. *J Neurotrauma* 27, 2091-2106.
34. Gensel, J. C., Tovar, C. A., Hamers, F. P., Deibert, R. J., Beattie, M. S., Bresnahan, J. C. (2006). Behavioral and histological characterization of unilateral cervical spinal cord contusion injury in rats. *J Neurotrauma* 23, 36-54.
35. Ma, M., Basso, D. M., Walters, P., Stokes, B. T., Jakeman, L. B. (2001). Behavioral and histological outcomes following graded spinal cord contusion injury in the C57Bl/6 mouse. *Exp Neurol* 169, 239-254.
36. Nishi, R. A., Liu, H., Chu, Y., Hamamura, M., Su, M. Y., Nalcioglu, O., Anderson, A. J. (2007). Behavioral, histological, and ex vivo magnetic resonance imaging assessment of graded contusion spinal cord injury in mice. *J Neurotrauma* 24, 674-689.

37. Kearney, P. A., Ridella, S. A., Viano, D. C., Anderson, T. E. (1988). Interaction of Contact Velocity and Cord Compression in Determining the Severity of Spinal Cord Injury. *J Neurotrauma* 5, 187–208.
38. Kraha, A., Turner, H., Nimon, K., Zientek, L.R., Henson, R.K. (2012). Interpreting multiple regression in the face of multi collinearity. *Frontiers in Psychology* 3, 1–10.
39. Ray-Mukherjee, J., Nimon, K., Mukherjee, S., Morris, D.W., Slotow, R., Hamer, M. (2014). Using commonality analysis in multiple regressions: a tool to decompose regression effects in the face of multicollinearity. *Methods in Ecology and Evolution* 5, 320–328.
40. Arani, A., Murphy, M. C., Glaser, K. J., Manduca, A., Lake, D. S., Jack, C.F., Jr, Ehman, R. L., Hudson, J., III (2015). Measuring the effects of aging and sex on regional brain stiffness with MR elastography in healthy older adults. *Neuroimage* 111, 59-64.
41. Elkin, B. S., Ilankovan, A., Morrison, B., III. (2010). Age-dependent regional mechanical properties of the rat hippocampus and cortex. *J Biomech Eng* 132, 011010-011010-10.
42. Clarke, E.C., Cheng, S., Bilston, L.E. (2009). The mechanical properties of neonatal rat spinal cord in vitro, and comparisons with adult. *Journal of Biomechanics* 42, 1397-1402.
43. Frostell, A., Hakim, R., Thelin, E. P., Mattsson, P., Svensson, M. (2016). A Review of the Segmental Diameter of the Healthy Human Spinal Cord. *Front Neurol* 7, 238.
44. Kameyama, T., Hashizume, Y., Sobue, G. (1996). Morphologic Features of the Normal Human Cadaveric Spinal Cord. *Spine* 21, 1285-1290.
45. Yu, Y. L., du Boulay, G. H., Stevens, J. M., Kendall, B. E. (1985). Morphology and measurements of the cervical spinal cord in computer-assisted myelography. *Neuroradiology* 27, 399-402.
46. Persson, C., McLure, S. W., Summers, J., Hall, R. M. (2009). The effect of bone fragment size and cerebrospinal fluid on spinal cord deformation during trauma: an ex vivo study. *J Neurosurg Spine* 10, 315-323.
47. Persson, C., Summers, J., Hall, R. M. (2011). The importance of fluid-structure interaction in spinal trauma models. *J Neurotrauma* 28, 113-125.

48. Bhatnagar, T., Liu, J., Yung, A., Cripton, P., Kozlowski, P., Tetzlaff, W., Oxland, T. (2016). Relating Histopathology and Mechanical Strain in Experimental Contusion Spinal Cord Injury in a Rat Model. *J Neurotrauma* 33, 1685-1695.
49. Sherman, J. L., Nassaux, P. Y., Citrin, C. M. (1990). Measurements of the normal cervical spinal cord on MR imaging. *AJNR Am J Neuroradiol* 11, 369-372.
50. Russell, C. M., Choo, A. M., Tetzlaff, W., Chung, T.-E. & Oxland, T. R. (2012). Maximum principal strain correlates with spinal cord tissue damage in contusion and dislocation injuries in the rat cervical spine. *J Neurotrauma*, 29, 1574–1585.
51. Khuyagbaatar, B., Kim, K. & Hyuk Kim, Y. (2014) Effect of bone fragment impact velocity on biomechanical parameters related to spinal cord injury: A finite element study. *J Biomechanics*, 47, 2820–2825.
52. Khuyagbaatar, B., Kim, K. & Kim, Y. H. (2015) Conversion Equation between the Drop Height in the New York University Impactor and the Impact Force in the Infinite Horizon Impactor in the Contusion Spinal Cord Injury Model. *J Neurotrauma*, 32, 1987–1993.

Table 1. Summary of biomechanical parameters of contusion injury. Direct measurements of peak force, impactor displacement from initial contact with the exposed dura and velocity at impact were recorded by a calibrated load cell located within the impactor tip and further analyzed using Labview software (National Instruments Corporation, Austin, TX) Impulse was calculated as the integral of force with respect to time.

Contusion parameter	Unit	Animal							Mean	SD	% variation
		#1	#2	#3	#4	#5	#6	#7			
Peak Force	<i>kdyne</i>	368 9	358 9	420 8	322 8	215 4	253 8	254 0	313 5	74 6	23.82
Displacement	<i>mm</i>	4.80	4.90	4.60	4.33	4.7 0	5.61	5.30	4.89	0.4 3	8.87
Impulse	<i>kdyne*s</i> <i>ec</i>	11.9 0	12.2 8	12.0 2	10.7 8	9.4 0	10.0 8	10.1 3	10.9 4	1.1 3	10.34
Velocity	<i>mm/sec</i>	188 6	186 8	186 1	170 6	156 0	179 8	179 7	178 2	11 5	6.48

SD: standard deviation.

Table 2. Body weight and ultrasound measures of spinal cord and CSF morphometry

Morphometric measures	Unit	Animal							Mean	SD	% variation
		#1	#2	#3	#4	#5	#6	#7			
Age	days	176	165	172	191	225	192	221	192	23.5	12.26
Body weight	kg	23.5	25.0	23.5	33.0	34.0	32.0	34.0	29.29	5.02	17.13
SC _{TR}	mm	6.54	6.33	6.62	7.04	6.92	6.85	6.58	6.70	0.25	3.71
SC _{DV}	mm	5.15	5.38	5.13	5.28	5.52	5.87	5.05	5.34	0.28	5.31
SC _{area}	mm ²	26.14	26.99	26.58	28.56	29.95	31.79	26.33	28.05	2.15	7.67
DS _{TR}	mm	8.31	7.88	8.15	7.96	8.46	8.62	9.23	8.37	0.46	5.50
DS _{DV}	mm	8.12	7.44	7.07	6.80	8.04	8.83	8.26	7.79	0.72	9.21
DS _{area}	mm ²	52.65	46.38	45.10	41.95	53.21	60.42	59.81	51.36	7.20	14.02
CSF _D	mm	2.47	1.03	1.03	0.73	1.02	1.29	2.15	1.39	0.66	47.28
CSF _V	mm	0.50	1.04	0.91	0.79	1.50	1.67	1.05	1.06	0.40	37.83

CSF_{DV}	<i>mm</i>	2.96	2.07	1.94	1.51	2.52	2.96	3.21	2.45	0.6 3	25.73
CSF_{area}	<i>mm</i> ²	26.5 1	19.3 8	18.5 2	13.3 9	23.2 5	28.6 3	33.4 8	23.31	6.8 2	29.24
CSF_D/CSF_V	<i>rati</i> <i>o</i>	4.98	0.99	1.13	0.93	0.68	0.78	2.04	1.65	1.5 4	93.28
SC_{area}/DS_{area}	<i>rati</i> <i>o</i>	0.50	0.58	0.59	0.68	0.56	0.53	0.44	0.55	0.0 8	13.65

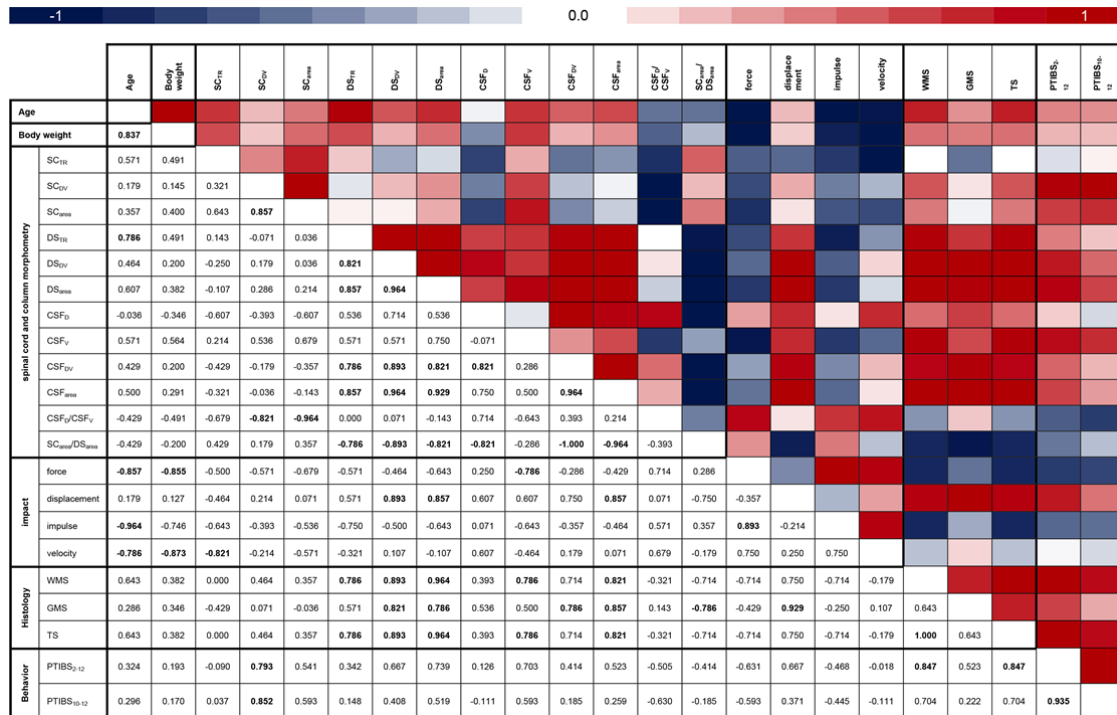
CSF_D: dorsal thickness of the CSF layer; CSF_V: ventral thickness of the CSF layer; SC_{DV}, dorso-ventral thickness of the spinal cord; SC_{TR}, transverse width of the spinal cord; DS_{TR}: transverse width of the dural sac; DS_{DV}: dorso-ventral thickness of the dural sac; SC_{area}: cross-sectional area of the spinal cord; DS_{area}: cross-sectional area of the dural sac; SC_{area}/DS_{area}: cross-sectional area of spinal cord to dural sac ratio. SD: standard deviation.

Table 3. The results of a principal components analysis (PCA) evaluating the relationship between all biomechanical, histological, and behavioral outcomes (n = 7). Loading magnitude is illustrated by the intensity of the color (Blue reflects negative and red reflects positive loadings). Loading values ≥ 0.80 or ≤ -0.8 are highlighted in white bold. PCA patterns revealed a three-factor structure that accounted for 92.08% of the variance in the data set. The first dimension (D1) accounted for 43.40 % of the variance in the dataset and showed high loadings for WMS, GMS, and TS and DS_{TR}, DS_{DV}, DS_{area}. D2 (25.25% of the variance) largely reflected high loadings for peak force, impulse, velocity, age, body weight and SC_{TR}. D3 accounted for 23.79% of the variance and indicated high loadings for PTIBS, SC_{DV} and SC_{area}.

		D1	D2	D3
Age		0.406	0.890	0.095
Body weight		0.185	0.873	0.094
Spinal cord and column morphometry	SC _{TR}	-0.418	0.803	0.164
	SC _{DV}	-0.058	0.105	0.966
	SC _{area}	-0.212	0.453	0.822
	DS _{TR}	0.807	0.522	-0.075
	DS _{DV}	0.960	0.066	0.213
	DS _{area}	0.904	0.245	0.334
	CSF _D	0.808	-0.391	-0.343
	CSF _V	0.440	0.447	0.628
	CSF _{DV}	0.974	0.022	-0.145
	CSF _{area}	0.993	0.114	0.009
	CSF _D /CSF _V	0.287	-0.540	-0.788
SC _{area} /DS _{area}	-0.974	-0.022	0.145	
Impact parameters	Force	-0.337	-0.756	-0.520
	Displacement	0.865	-0.156	0.311
	Impulse	-0.374	-0.842	-0.298
	Velocity	0.186	-0.964	-0.129
Histology	WMS	0.796	0.283	0.504
	GMS	0.846	-0.007	0.126
	TS	0.796	0.283	0.504
Behavior	PTIBS ₂₋₁₂	0.522	0.008	0.837
	PTIBS ₁₀₋₁₂	0.261	0.048	0.884

CSF_D: dorsal thickness of the CSF layer; CSF_V: ventral thickness of the CSF layer; SC_{DV}, dorso-ventral thickness of the spinal cord; SC_{TR}, transverse width of the spinal cord; DS_{TR}: transverse width of the dural sac; DS_{DV}: dorso-ventral thickness of the dural sac; SC_{area}: cross-sectional area of the spinal cord; DS_{area}: cross-sectional area of the dural sac; SC_{area}/DS_{area}: cross-sectional area of spinal cord to dural sac ratio; PTIBS₂₋₁₂: average “Porcine Thoracic Behavior Scale” score over week 2 till 12 post SCI; PTIBS₁₀₋₁₂: average “Porcine Thoracic Behavior Scale” score over week 10 till 12 post SCI.

Table 4. Non-parametric Spearman correlations (*r*) between spinal cord morphometry measures, impact parameters and post-SCI histological and functional outcome. Values and shading intensities represent spearman rank correlation coefficients between two variables. Values in bold are different from 0 with a significance level of * $p \leq 0.05$ or ** $p \leq 0.005$. CSF_D: dorsal thickness of the CSF layer; CSF_V: ventral thickness of the CSF layer; SC_{DV}, dorso-ventral thickness of the spinal cord; SC_{TR}, transverse width of the spinal cord; DS_{TR}: transverse width of the dural sac; DS_{DV}: dorso-ventral thickness of the dural sac; SC_{area}: cross-sectional area of the spinal cord; DS_{area}: cross-sectional area of the dural sac; SC_{area}/DS_{area}: cross-sectional area of spinal cord to dural sac ratio.



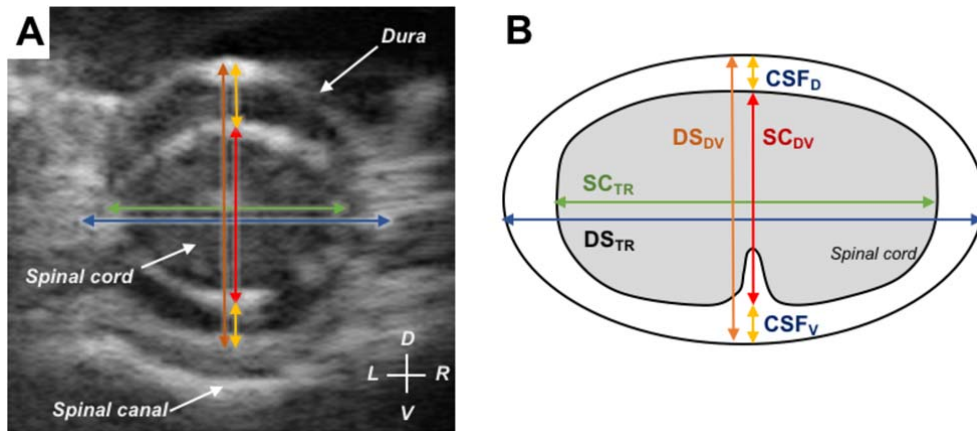


Figure 1. Pre-operative ultrasound images used to generate morphometric measures of the spinal cord and cerebrospinal fluid (CSF) space. (A). Axial ultrasound image of the pig spinal cord at the T10 level prior to SCI. **(B)** Measurement of the various cord parameters analysed. CSF_D : dorsal thickness of the CSF layer; CSF_V : ventral thickness of the CSF layer; SC_{DV} , dorso-ventral thickness of the spinal cord; SC_{TR} , transverse width of the spinal cord; DS_{TR} : transverse width of the dural sac; DS_{DV} : dorso-ventral thickness of the dural sac.

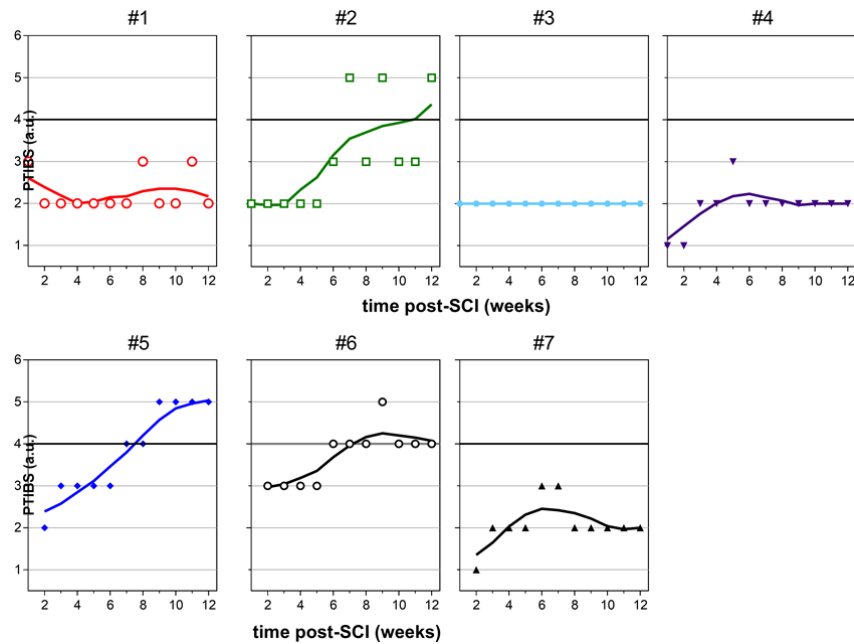


Figure 2. Assessment of functional recovery over the 12 week study period using the Porcine Thoracic Injury Behavior Scale (PTIBS). Variability in PTIBS measures is found between *animals* (#1-7), but also for *individual animals* tested on different weeks (2-12 weeks post-SCI). The solid line in each graph represents the estimated smooth curve for each animals.

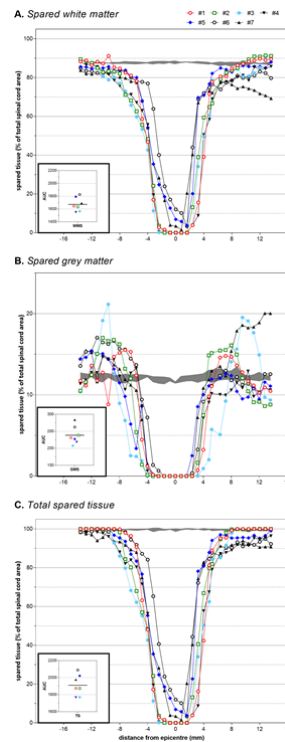


Figure 3. Spinal cord lesion at 12 weeks post-injury, quantified as the percentage of white, gray and total matter spared tissue around the injury site. Percentage spared (A) grey matter, (B) white matter and (C) total tissue (the summation of spared white and gray matter) determined by area measurements taken from axial sections of spinal cord tissue 800 μm apart. Each line in the graph represents an individual SCI animal (#1-7). SHAM (surgically exposed but not subjected to the SCI procedure)¹⁸ control measures were included to represent normal “uninjured” values (grey shading; mean \pm SEM).

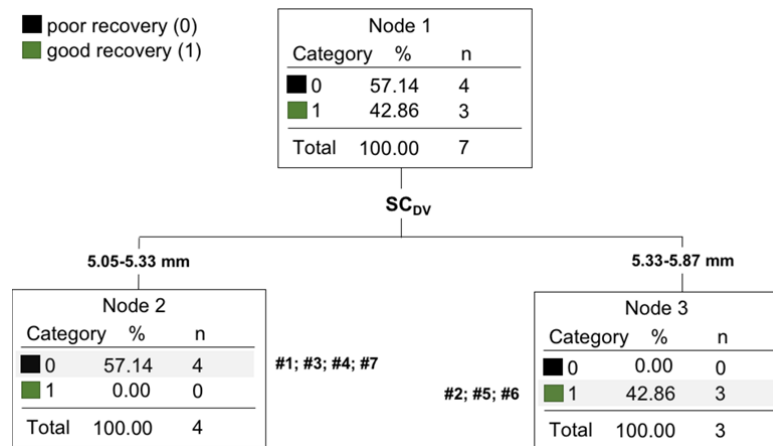


Figure 4. Classification and regression tree (CART) analysis to predict behavioral recovery. Analysis identified a decision tree defined by three nodal points that stratified the cohort into two groups. The tree showed that the proximal split was based on SC_{DV} . With a cut-off to be 5.331 mm, 100% correct *classification into two target groups*: those animals whose PTIBS scores remained ≤ 3 by the final week of the study (i.e. poor recovery; #1,3,4,7) and those who recovered from the initial deficit fairly well to a PTIBS of 4-5 (i.e. good recovery; animal #2, #5, #6).

Supplementary Table 1. Intra- and inter-observer reliability, shown by the intra-class correlation coefficient (ICC), for the Pre-SCI ultrasound analysis on CSF space and spinal cord dimensions. Parameters were found to be highly reliable for both intra- and inter-observer assessment, with *ICC values* between 0.83 and 1.00.

Parameters	Intra-observer ICC*		Inter-observer ICC*
	Observer 1	Observer 2	
	<i>Mean (95% CI)</i>	<i>Mean (95% CI)</i>	<i>Mean (95% CI)</i>
SC _{TR}	0.94 (0.89–0.96)	0.93 (0.88–0.96)	0.93 (0.88–0.96)
DS _{TR}	0.94 (0.89–0.96)	0.93 (0.89–0.95)	0.93 (0.89–0.95)
SC _{DV}	0.99 (0.98–1.00)	0.99 (0.98–1.00)	0.98 (0.97–0.99)
DS _{DV}	0.99 (0.98–1.00)	0.99 (0.98–1.00)	0.98 (0.97–0.99)
CSF _V	0.97 (0.94–0.99)	0.97 (0.93–0.99)	0.97 (0.93–0.99)
CSF _D	0.97 (0.93–0.99)	0.97 (0.93–0.99)	0.96 (0.93–0.99)
SC _{area}	0.93 (0.84–0.98)	0.97 (0.93–0.99)	0.94 (0.89–0.97)
DS _{area}	0.92 (0.83–0.98)	0.95 (0.86–0.99)	0.93 (0.89–0.98)

CSF_D: dorsal thickness of the CSF layer; CSF_V: ventral thickness of the CSF layer; SC_{DV}, dorso-ventral thickness of the spinal cord; SC_{TR}, transverse width of the spinal cord; DS_{TR}: transverse width of the dural sac; DS_{DV}: dorso-ventral thickness of the dural sac; SC_{area}: cross-sectional area of the spinal cord; DS_{area}: cross-sectional area of the dural sac; ICC: intra-class correlation coefficient of absolute agreement of single measures; CI: confidential interval; * All data were significant at $p < 0.001$.